J Appl Electrochem (2009) 39:1199–1205
DOI 10.1007/s10800-009-9785-6

ORIGINAL PAPER

Dodigen 213-N as corrosion inhibitor for ASTM 1010 mild steel in 10% HCL

M. F. L. Granero · P. H. L. S. Matai · I. V. Aoki · I. C. Guedes

Received: 13 October 2008 / Accepted: 24 December 2008 / Published online: 14 February 2009

Abstract This article describes a study of the behavior of a mixture of amines and amides, commercially known as Dodigen 213-N (D-213 N), as a corrosion inhibitor for ASTM 1010 mild steel in 10% w/w HCl solution. The concentration range used was 1×10^{-5} M to 8×10^{-4} M. The weight loss and electrochemical techniques used were corrosion potential measurement, anodic and cathodic polarization curves, and electrochemical impedance spectroscopy (EIS). The solution temperature was 50 ± 1 °C and it was naturally aerated. The corrosion potential values shifted to slightly more positive values, thus indicating mixed inhibitor behavior. The anodic and cathodic polarization curves showed that D-213 N is an effective corrosion inhibitor, since both the anodic and the cathodic reactions were polarized in comparison with those obtained without inhibitor. For all concentrations the cathodic polarization curves were more polarized than the anodic ones. The inhibition efficiency was in the range 75–98%, calculated from values of weight loss and corrosion current density, i_{corr}, obtained by extrapolation of Tafel cathodic linear region.

Keywords Amide and amine mixture · Corrosion inhibitor · Hydrochloric acid and mild steel

M. F. L. Granero · P. H. L. S. Matai · I. V. Aoki · I. C. Guedes (✉)
Departamento de Engenharia Química da Escola Politécnica da, Universidade de São Paulo, 61.548, São Paulo, SP 05424-970, Brazil
e-mail: icguedes@usp.br

1 Introduction

Carbon steel is a common constructional material for many industrial units because of its cost and excellent mechanical properties. However, it suffers severe attack in service, particularly in oil and gas production systems [1].

Corrosion is a major problem in oil and gas production. The type and extent of this problem depend on fluid composition, such as the oil type, oil/water ratio, water salinity, gas type, and gas content [2]. The main gases that affect metal corrosion in petroleum are hydrogen sulfide, carbon dioxide, and oxygen [3]. The combination of hydrogen sulfide and carbon dioxide is more aggressive than hydrogen sulfide alone [4]. The salinity of water affects the solubility of the gases, which influences the corrosivity of the environment. The presence of sodium chloride in concentrations of up to 1 wt% increases the corrosion rate, because it prevents the formation of a protective FeS film on the mild steel surface [5].

Many organic compounds containing oxygen, nitrogen, and sulfur atoms have been used as corrosion inhibitors for carbon steel in various aggressive environments [6–9]. The addition of high-molecular-weight organic compounds such as surfactants to combat corrosion of carbon steel has found wide application in many fields [1].

Surfactant exerts its inhibition effect by adsorption ability, which is affected by definite physical–chemical characteristics of the surfactant molecule such as functional groups, aromaticity, π-orbital character of the donating electrons, steric effect, and the electronic structure of the molecule [10].

Depending upon the concentration of the surfactant, adsorption may occur as an individual molecule or as surfactant aggregates of various types [11].

A very important factor in the corrosion process is the presence of sulfur compounds and calcium and magnesium chlorides, besides the impurities in the raw oil fed to petroleum refining [12–14]. The presence of chloride ions can produce hydrochloric acid at the top of distillation columns, leading to corrosion.

Amines are well known as corrosion inhibitors for iron and its alloys. The relative high water solubility of low-molecular-weight amines is an advantage for their use as inhibitors [15, 16]. The presence of a heteroatom in an organic compound with unsaturated π-bonds causes adsorption on the metal surface, which reduces metal dissolution [17].

The aim of this work is to study the efficiency of a mixture of amides and amines as corrosion inhibitor and their adsorption behavior in aqueous 10% hydrochloric acid solutions for ASTM 1010 mild steel.

2 Experimental

Samples of ASTM 1010 mild steel with the following chemical composition (wt%): 0.098 C; 0.02 Mn, 0.03 Si, 0.015 P, 0.06 Cu, 0.016 Ni, 0.036 Al, 0.011 S, and balance Fe were employed. The industrial formulation used as corrosion inhibitor is named Dodigen 213-N (D-213 N).

D-213 N in the concentration range 1×10^{-5} M to 8×10^{-4} M was used. A 10% w/w hydrochloric acid aqueous solution was used as aggressive medium.

2.1 Infrared (IR) spectroscopy

The purpose of IR spectroscopy was to identify the organic functional groups present in the industrial formulation studied. BOMEN MB-100 spectrophotometer was used to record the spectrum in the 4,000–400 cm^{-1} range. The original concentrated inhibitor sample was analyzed in a flat plate ZnS crystal.

2.2 Weight loss experiments

Mild steel (ASTM 1010) samples were cut to approximately $18 \times 10 \times 3$ mm dimensions. The specimens, working electrodes, were mechanically polished with different grades of emery paper 320, 400, and 600 grit, sequentially, washed with distilled water, rinsed with ethanol and acetone, and dried in a hot air stream. They were weighed before and after immersion in 10% w/w HCl naturally aerated solution at a controlled temperature of 50 °C, in presence and absence of inhibitor for 2 h. The corrosion rate was determined in the absence and presence of corrosion inhibitor. Subsequently, the coverage degree, θ, was obtained using

$$\theta = \frac{v_{\text{corr, 0}} - v_{\text{corr, i}}}{v_{\text{corr, 0}}},$$

where $v_{\text{corr,0}}$ and $v_{\text{corr,i}}$ are the corrosion rate in the absence and presence of the inhibitor, respectively.

2.3 Electrochemical techniques

The electrochemical techniques employed were corrosion potential (E_{corr}) monitoring, anodic and cathodic polarization curves, and electrochemical impedance spectroscopy. Mild steel (ASTM 1010) specimens were cut in disk form and submitted to the same surface treatment described above for the weight loss experiments. They were put in a special holder in order to expose a 1 cm^2 area. The tests were performed in a Voltalab 40 radiometer potentiostat provided with a frequency response analyzer (FRA) in a glass cell supporting 350 mL electrolyte (10% w/w HCl) at a temperature of 50 °C with Ag/AgCl (KCl sat.) as a reference electrode provided with a Luggin capillary bridge arrangement to minimize ohmic polarization and a Pt foil as the counter electrode. The electrode was immersed in the corrosive medium for 90 min and the corrosion potential was automatically recorded. The electrochemical impedance spectra were obtained in a frequency range from 10 kHz to 100 mHz. Disturbance amplitude of 10 mV was applied relative to open-circuit potential and ten measurements were performed for each frequency decade. After the electrochemical impedance spectrum was obtained, the anodic and cathodic polarization curves were run. The potential range studied was from −1,000 mV to 100 mV versus Ag/AgCl, with 1 mV s^{-1} scan rate. All the techniques were conducted with static working electrodes, naturally aerated electrolytes at a controlled temperature of 50 ± 1 °C, and in absence and presence of D-213 N inhibitor. All the solutions used were prepared from reagent-grade chemicals and distilled water.

3 Results and discussion

3.1 Infrared spectrum

Figure 1 shows the IR spectrum and Table 1 presents the peaks wavenumbers (cm^{-1}) observed for the sample of D-213 N. The peaks and their respective attribution [18] are: 3,550–3,150 cm^{-1}, showing the axial deformation of N–H groups for aliphatic primary amine; 1,461 cm^{-1}, corresponding to the symmetric angular deformation of the CH_2 group in primary amines; 1,303 cm^{-1}, a strong band corresponding to aromatic primary amines; 1,108 cm^{-1} from the axial deformation of the C–N group of primary aliphatic amines; and 824.5 cm^{-1} for the symmetric angular

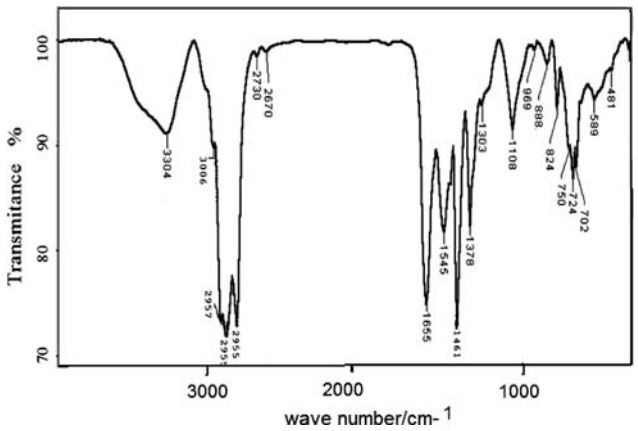

Fig. 1 Infrared spectrum for Dodigen 213 N inhibitor

out-of-plane deformation for the N–H group of amides. The presence of peaks at 1,546 cm^{-1} and 1,655 cm^{-1} indicates the presence of amines and the peak at 724 cm^{-1} corresponds to the presence of long-chain hydrocarbons. The IR spectrum indicates that the analyzed sample is probably a mixture of aliphatic primary amines, primary amides, aromatic amines, and a hydrocarbon solvent [18].

3.2 Weight loss experiments

Based on the results obtained from weight loss measurements, the inhibitor degrees of coverage on ASTM 1010 mild steel were calculated and are presented in Table 2. The results show that D-213 N acts as a corrosion inhibitor for mild steel in 10% w/w HCl solution. When D-213 N is present, the obtained corrosion rate is lower than that observed in the absence of D-213 N inhibitor.

The best trend line and related statistical parameters, such as determination coefficient R^2 and standard deviation for linear and angular coefficients, were obtained by fitting coverage degree results to Langmuir (Eq. 1) adsorption isotherm.

Table 2 Corrosion rates (v_{corr}) and coverage degrees (θ) for ASTM 1010 mild steel in 10% w/w HCl solutions in presence of D-213 N inhibitor

D-213 N concentration/M	v_{corr}/mg cm^{-2} h^{-1}	θ
0.0	23.2 ± 0.30	0.00
1.0×10^{-5}	22.4 ± 0.70	0.04
2.0×10^{-5}	21.3 ± 0.10	0.08
4.0×10^{-5}	18.6 ± 0.30	0.20
5.0×10^{-5}	9.2 ± 0.20	0.60
6.0×10^{-5}	8.7 ± 0.20	0.62
8.0×10^{-5}	7.5 ± 0.50	0.68
1.0×10^{-4}	5.6 ± 0.10	0.76
3.0×10^{-4}	3.6 ± 0.30	0.84
7.0×10^{-4}	1.9 ± 0.40	0.92
8.0×10^{-4}	1.1 ± 0.10	0.95

Table 1 Infrared spectroscopy spectrum peak wavenumbers (cm^{-1}) for D-213 N corrosion inhibitor

Wave number/cm^{-1}	Peak correspondence	Observation
589	Aromatic amine	
724	CH_2 angular deformation (out or plan)	Appears for long hydrocarbon chains
750	Aromatic amine	
824	N–H deformation for amines and amides	
1,108	Medium-intensity band corresponding to aliphatic primary amines	
1,303	Strong-intensity band corresponding to aromatic primary amines	
1378	Symmetric angular deformation on the CH_3 plane	
1,461	Symmetric angular deformation on the CH_2 plane	
1546	Angular deformation of N–H for primary amines	
1,655	High-intensity peak for the primary amines	
2,855	Symmetric axial deformation for CH_2	Appears for long hydrocarbon chains
2925	Asymmetric axial deformation for CH_2	Appears for long hydrocarbon chains
2,957	Asymmetric axial deformation for CH_3	Appears for long hydrocarbon chains
3,006	Peak corresponding to the aromatic rings	
3,150–3,550	Asymmetric axial deformation of N–H for the primary amines	

Table 3 Statistical results obtained from the linear regression analysis and parameters for the Langmuir adsorption isotherm for ASTM 1010 mild steel in 10% w/w HCl solutions for different concentrations of D-213 N corrosion inhibitor

Parameter	Langmuir isotherm
Corresponding equation	$\theta/(1-\theta) = k^*C$
Determination coefficient, R^2	0.97
Linear coefficient $\pm$ σ	0.30 $\pm$ 0.13
Angular coefficient $\pm$ σ	(4.3 $\pm$ 0.14) $\times$ 10^4

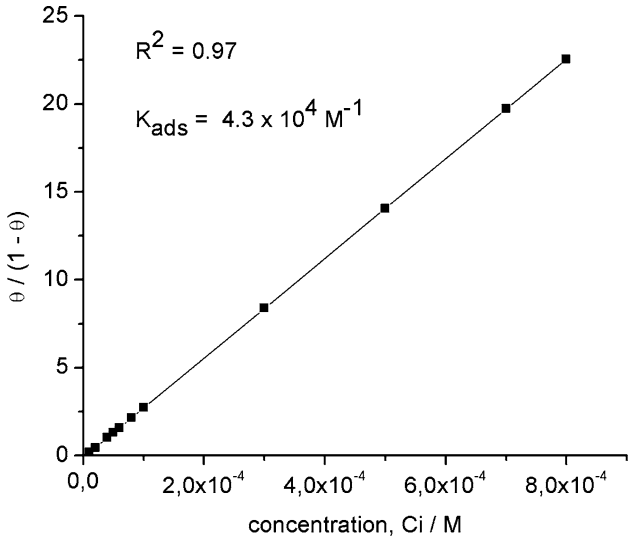

Fig. 2 Langmuir adsorption isotherm for D-213 N corrosion inhibitor on ASTM 1010 mild steel in 10% w/w HCl solution

$$\theta/(1-\theta) = k^*C, \quad (1)$$

where θ is the fractional coverage degree, k is the adsorption constant, and C is the adsorbate concentration.

Results of the statistical isotherm equation parameters are given in Table 3. Figure 2 shows the Langmuir adsorption isotherm.

The angular coefficient of Langmuir adsorption isotherm represents the adsorption equilibrium constant, k_{ads}. Its value is $k_{ads} = 4.3 \times 10^4$ M^{-1}. This value can be used to calculate the standard adsorption free energy, which provides

$$K_{ads} = \frac{1}{55.5}\exp -\left(\frac{\Delta G^0_{ads}}{RT}\right).$$

So, $\Delta G^0_{ads} = -RT\ln(55.5K_{ads})$, where the value 55.5 is the water concentration in the solution in mol L^{-1}, R is the gas constant (8.3147 J mol^{-1} K^{-1}), T is the absolute temperature, and ΔG^0_{ads} is the standard free adsorption energy [8]. So, $\Delta G^0_{ads} = -36.4$ kJ mol^{-1}. This value in modulus is higher than the minimum value of 25.2 kJ mol^{-1} for chemical adsorption, so it can be concluded that chemical adsorption takes place [19].

The free energy involved in the adsorption is an important factor related to the high efficiency of a substance as an inhibitor. When an inhibited solution contains absorbable anions, such as chloride ions, they are specifically adsorbed on the metal surface by creating oriented dipoles, thereby increasing the adsorption of the organic cations over them [20], and this may be the way D-213 N inhibitor is adsorbed on the steel [21–23].

3.3 Electrochemical techniques

3.3.1 Corrosion potential

Table 4 shows the corrosion potential results for ASTM 1010 mild steel in 10% w/w HCl solution in absence and presence of increasing D-213 N inhibitor concentrations.

For all the inhibitor concentrations studied, the corrosion potentials shifted to slightly more negative values in comparison with values obtained in the absence of D-213 N inhibitor. This slight variation in the corrosion potential indicates its mixed inhibition behavior.

3.3.2 Anodic and cathodic polarization curves

Figure 3 presents the anodic and cathodic polarization curves obtained for ASTM 1010 mild steel in 10% w/w HCl solution. Both anodic and cathodic curves were polarized in comparison with that obtained in the absence of inhibitor, thus inhibiting both the anodic dissolution of mild steel and the reduction of hydrogen ions on the metal

Table 4 Corrosion potential (E_{corr}), corrosion current densities (i_{corr}), and efficiencies (η) from gravimetric tests and polarization curves for ASTM 1010 mild steel in 10% w/w HCl solutions for different concentrations of D-213 N corrosion inhibitor

Electrochemical techniques				Gravimetric technique	
Concentration D-213 N/M	E_{corr}/mV	i_{corr}/A cm^{-2}	η/%	i_{corr}/A cm^{-2}	η/%
0.00	−350	2.0 $\times$ 10^{-2}	–	2.2 $\times$ 10^{-2}	–
1.0 $\times$ 10^{-4}	−380	5.1 $\times$ 10^{-3}	74.0	5.4 $\times$ 10^{-3}	75.0
5.0 $\times$ 10^{-4}	−388	1.6 $\times$ 10^{-3}	92.0	1.8 $\times$ 10^{-3}	92.0
7.0 $\times$ 10^{-4}	−392	4.0 $\times$ 10^{-4}	98.0	1.1 $\times$ 10^{-3}	95.0

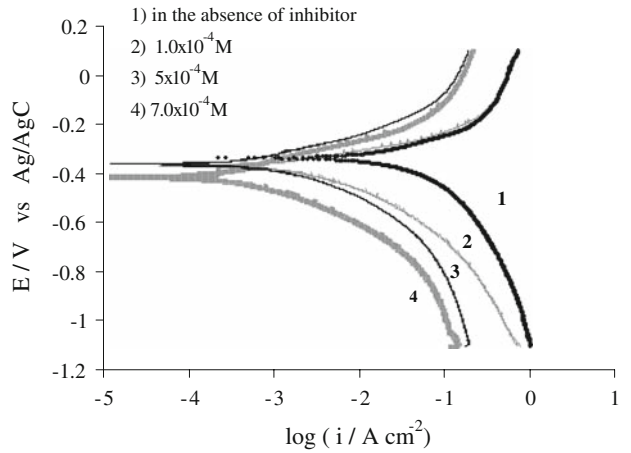

Fig. 3 Polarization curves for ASTM 1010 mild steel in 10% w/w HCl solution: (1) in the absence of D-213 N inhibitor, (2) in the presence of 1×10^{-4} M, (3) in the presence of 5×10^{-4} M, and (4) in the presence of 7×10^{-4} M

surface. This confirms that D-213 N behaves as a mixed inhibitor.

Table 4 shows the results for the corrosion potential, corrosion current density, and inhibition efficiency for ASTM 1010 mild steel obtained from weight loss measurements and polarization curves in 10% w/w HCl in absence and presence of increasing D-213 N inhibitor concentrations.

The results obtained from the weight loss measurements and from the polarization curves are in close agreement. The corrosion current densities decrease markedly for higher inhibitor concentrations. The inhibition efficiency values are nearly the same for both techniques. This confirms the importance of using more than one technique to obtain the results [24].

3.3.3 Electrochemical impedance spectroscopy

Figure 4 shows the EIS diagrams for ASTM 1010 mild steel in 10% w/w hydrochloric acid solution in absence and presence of D-213 N inhibitor. The Nyquist diagrams (Fig. 4a) show higher resistances to charge transfer as the concentration of D-213 N inhibitor increases.

In order to analyze the Nyquist plots more concisely, equivalent circuits were proposed for data interpretation. For all measurements, the equivalent circuit model represented in Fig. 5 was used.

C_{dl} is the double-layer capacitance and R_{ct} represents the resistance of the interfacial charge transfer reaction. These two parameters represent the electrochemical behavior of the steel surface. To take into account the nonideal behavior of the capacitive elements C_{dl}, a constant phase element (CPE) was introduced into the model. The impedance of such an element can be written as follows:

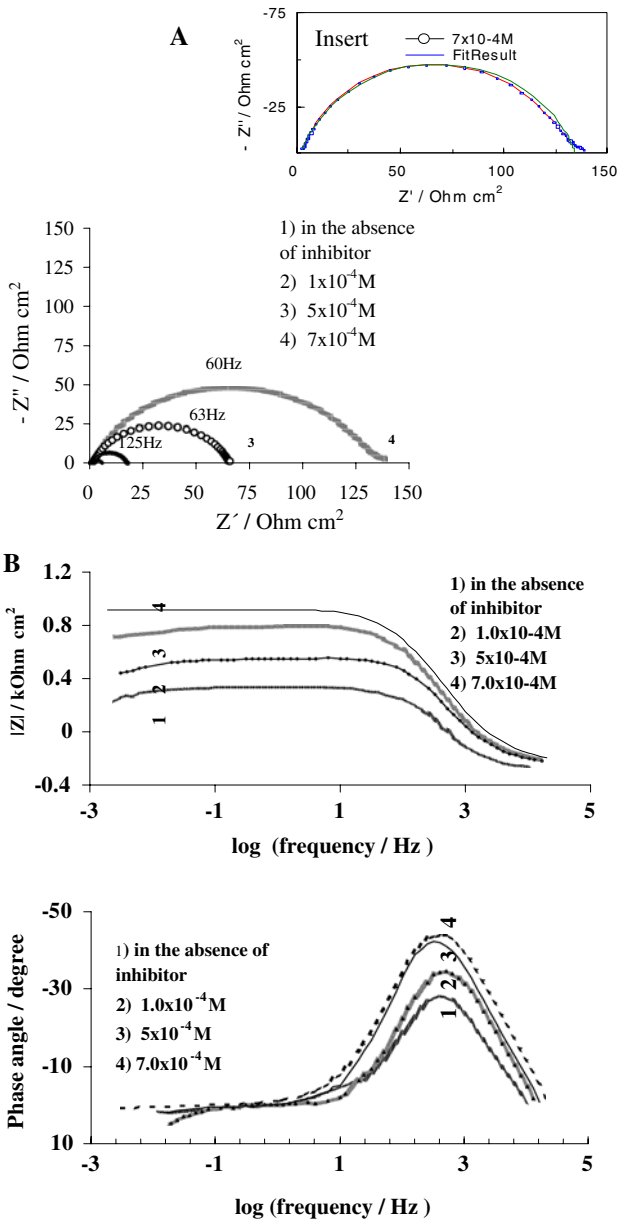

Fig. 4 **a** Nyquist diagrams for ASTM 1010 mild steel in 10% w/w HCl solution: (1) in the absence of D-213 N inhibitor, (2) in the presence of 1×10^{-4} M, (3) in the presence of 5×10^{-4} M, and (4) in the presence of 7×10^{-4} M. **b** Bode diagrams for ASTM 1010 mild steel in 10% w/w HCl solution: (1) in the absence of D-213 N inhibitor, (2) in the presence of 1×10^{-4} M, (3) in the presence of 5×10^{-4} M, and (4) in the presence of 7×10^{-4} M

$$Z_{\mathrm{CPE}} = \frac{1}{(j\omega)^n y_0}.$$

The values of the CPE parameters y_0 and n were determined through a fitting procedure and the capacitance C could then be derived with the equation proposed by Hsu and Mansfeld [25].

$$C = y_0 \left(\omega''_m\right)^{n-1}$$

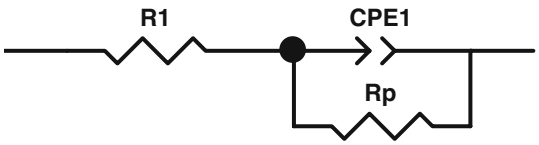

Fig. 5 Electrical equivalent circuit model proposed to simulate the impedance behavior of steel in hydrochloric acid in presence and absence of D-213 N inhibitor

where $y_0 = \mathrm{CPE}_1 - T$, and $n = \mathrm{CPE}_1 - P$ (in Zview software) and $\omega''_m = f_{max}$ is the frequency at which the imaginary part of the measured impedance has a maximum. These results are presented in Table 5.

Polarization curves (Fig. 3) and EIS results (Fig. 4a, b) consistently indicate that D-213 N inhibitor protects the surface from corrosion. This is indicated by the increase in charge transfer resistance and the decrease in double-layer capacitance, which are in turn the consequence of the participation of D-213 N inhibitor in the protective layer.

It is also observed that the frequency of the maximum point of the capacitive arc is smaller for higher concentrations of D-213 N inhibitor. The diameter of the capacitive arcs increase for increasing concentrations of the studied molecule as corrosion inhibitor, reaching a maximum diameter at the concentration of 7.0×10^{-4} M, indicating that the charge transfer process between the metal and the solution becomes less intense in the presence of higher inhibitor concentrations. These results are also confirmed by the Bode diagrams (Fig. 4b), which show that the impedance of the system at low frequencies (resistance to charge transfer) becomes higher as the concentration of D-213 N inhibitor increases, which is probably associated with the formation of a more protective film on the steel surface [17]. Finally, it can be concluded that the D-213 N inhibitor acts as an effective corrosion inhibitor for ASTM 1010 carbon steel in HCl w/w 10%.

Table 5 shows the values obtained for the charge transfer resistance (R_{ct}) and double-layer capacitance (C_{dl}) in absence and presence of different concentrations of D-213 N inhibitor. The values of R_{ct} increase with increasing inhibitor concentration, indicating that metal/electrolyte interface reactions are more difficult for higher concentrations of D-213 N inhibitor. On the other hand, the values of C_{dl} diminish, which is probably due to formation of a barrier on the surface of the mild steel that minimizes ion exchange through the double layer on the metal/electrolyte interface. In Fig. 4b, Bode diagrams show that the values of the impedance modulus and phase angle also increase gradually with increasing inhibitor concentration, indicating the formation of a protective film. These results confirm that the absorbed film formed by D-213 N inhibitor in 10% HCl solution becomes more protective for higher D-213 N concentrations.

Table 5 Parameters obtained from the fitting process of EIS results with the equivalent circuit model in Fig. 5, for ASTM 1010 mild steel in 10% w/w HCl solutions for different concentrations of D-213 N corrosion inhibitor

D-213 N inhibitor concentration/M	y_0	n	R_{ct}/kΩ cm^2	$C_{dl} = y_0(\omega''_m)^{n-1}$/μF cm^{-2}
0.0	0.0011078	0.80	5.5	320
1.0×10^{-4}	0.000640	0.81	6.3	256
5.0×10^{-4}	0.000147	0.79	64.4	30
7.0×10^{-4}	0.000064	0.79	132.6	27

4 Conclusions

The following conclusions can be drawn:

1. The IR spectrum indicates that the sample analyzed is probably a mixture of aliphatic primary amines, primary amides, aromatic amines, and a hydrocarbon solvent.
2. The Langmuir adsorption isotherm presents a good fit to coverage degree, indicating that only one chemical adsorbed layer is formed.
3. For all the concentrations and techniques studied, the results indicate that D-213 N acts as an effective mixed corrosion inhibitor for ASTM 1010 mild steel in 10% w/w HCl.
4. EIS results confirm the presence of the adsorbed D-213 N corrosion inhibitor in the metal/electrolyte interface, evidenced by higher impedance modulus and phase angles for increasing inhibitor concentrations.
5. The results from all the techniques employed to assess the behavior of D-213 N are in close agreement, indicating the protection against corrosion provided by this inhibitor.

Acknowledgements The authors gratefully acknowledge CNPq for financial support.

References

1. Alsabagh AM, Migahed MA, Hayam SA (2006) Reactivity of polyester aliphatic amine surfactant as corrosion inhibitors for carbon steel in formation water (deep well water). Corros Sci 48:813
2. Rozenfeld IL (1981) Corrosion inhibitors. McGraw-Hill, New York
3. Al-Hajji JN, Reda MR (1993) Behavior of low-residual. Carbon steels in a sour environment. Corrosion 49:363
4. Tuttle RN, Kane RD (1981) H2S corrosion in oil and gas petroleum–a compilation of classic papers. NACE, Houston, TX

5. Efird KD, Jasinski RJ (1989) The effect of the crude oil on the corrosion of steel in crude oil/brine production. Corrosion 45:63
6. Kaddouri M, Cheriaa N, Souane R, Bouklah M, Aouniti A, Abidi R, Hammouti B, Vicens J (2008) Novel calixarene derivatives as inhibitors of mild C-38 steel corrosion in 1 M HCl. J Appl Electrochem 38:1253–1258
7. Prabhu A, Shanbhag AV, Venkatesha TV (2007) Influence of tramadol [2-[(dimethylamino)methyl]-1-(3-methoxyphenyl) cyclohexanol hydrate] on corrosion inhibition of mild steel in acidic media. J Appl Electrochem 37:491497
8. Bastidas JM, Polo JL, Cano E (2000) Substitutional inhibition mechanism of mild steel hydrochloric acid corrosion by hexylamine and dodecylamine. J Appl Electrochem 30:1173–1177
9. Shanbhag AV, Venkatesha TV, Prabhu RA, Kalkhambkar RG, Kulkarni GM (2008) Corrosion inhibition of mild steel in acidic medium using hydrazide derivatives. J Appl Electrochem 38: 279–287
10. Migahed MA (2005) Electrochemical investigation of the corrosion behaviour of mild steel in 2 M HCl solution in presence of 1-dodecyl-4-methoxy pyridinium bromide. Mater Chem Phys 93:48
11. Rafiquee MZA, Saxena N, Khan S, Quraishi MA (2008) Influenceof surfactantson the corrosio ninhibition behaviour of 2-aminophenyl-5-mercapto-1-oxa-3, 4-diazole(AMOD) on mild steel. Mat Chem Phys 93:528
12. White RA, Ehmke EF (1991) Materials Selection for Refineries and Associated Facilities. NACE-National Association of Corrosion Engineers, Houston, TX
13. Ashassi-Sorkhabi H, Majidi MR, Seyyedi K (2004) Investigation of inhibition effect of some amino acids against steel corrosion in HCl solution. Appl Surf Sci 225:176
14. Martinez S, Stern I (2002) Thermodynamic characterization of metal dissolution and inhibitor adsorption processes in the low carbon steel/mimosa tannin/sulfuric acid system, Appl Surf Sci 199:83
15. Braun RD, Lopez EL, Vollmer DP (1993) Low molecular weight straight-chain amines as corrosion inhibitors. Corros Sci 34:1251
16. Szauer T, Brandt A (1981) Adsorption of oleates of various amines on iron in acidic solution. Electrochim Acta 26:1209
17. Srhiri A, Etman M, Dabosi F (1996) Electro and physicochemical study of corrosion inhibition of carbon steel in 3% NaCl by alkylimidazoles. Electrochim Acta 41:429
18. Silverstein RM, Bassler GC, Morill TC (1976) Spectrometric identification of organic compounds. Wiley, New York
19. Castellan GW (1984) Physical Chemistry, 2nd edn. Addison-Wesley, MA, USA
20. Frignani A, Trabanelli G, Zucchi F, Zucchini M (1980) 5th European symposium on corrosion inhibitors, Ann. Univ. Ferrara, N. S. Sez. V Suppl **7** p 1185
21. El-Awady AA, Abd-El-Nabey BA, Asís SG (1992) Kinetic-thermodynamic and adsorption isotherms analices for the inhibition of the acidcorrosion of steel by cyclic and open–chain amines. J Electrochem Soc 139:2149
22. Guedes IC PhD thesis (1996) Eficiência dos inibidores de corrosão benzotriazol, N-feniltiouréia e cloreto de hexadeciltrimetil amônio quaternário para ferro puro, aço carbono e aço ARBL em meio de ácido sulfúrico.Escola Politécnica da Universidade de São Paulo, 178p
23. Guedes IC, Maranhão SLA, Aoki IV (2002) Copper phthalocyanine as corrosion inhibitor for ASTM A606–4 steel in 16% hydrochloric acid. J Appl Electrochem 32:915
24. Guedes IC, Taqueda MES, Aoki IV (1998) Polarisation curves and experiment design as tools in the search of optimized inhibitors mixture formulation for HSLA steel in hydrochloric acid. Mater Sci Forum 237:289
25. Hsu CH, Mansfeld F (2001) Concerning the conversion of the constant phase element parameter Y_0 into a capacitance. Corrosion 57:747